

**R2E-related MD: slow controlled losses for RadMon/BLM cross-checks**

M. Calviani (EN/STI), M. Brugger (EN/STI), G. Spiezia (EN/STI), M. Sapinski (BE/BI), A. Priebe (BE/BI), A. Nordt (BE/BI), M. Pojer (BE/OP)

Keywords: R2E, RadMon, BLM, injection, dump, SEU, dose

---

**Summary**

The purpose of the dedicated R2E MD has been to evaluate the R factor (i.e. the ratio between the thermal neutron fluence and the high energy hadron fluence (>20MeV) for various tunnel locations, to measure the HEH radiation level gradient along the MBC dipole and on the MQ, to check the ratio the BLM measured dose and RadMon SEU counts and to study the dose gradient between the standard BLM beam axis location and at the level of the equipment location. Within the R2E Mitigation Project, these accurate measurement and cross-check of the mentioned parameters are of great importance for the evaluation and interpretation of the R2E-related radiation levels, as well as for the evaluation of the failure cross-section of specific equipment (i.e. QPS ISO150). In addition, a short part of the MD has been devoted to the comparison of BLM signals generated by loss directed inwards and outwards with respect to the LHC ring.

---

**1. Introduction and motivation for an R2E-dedicated MD**

The present MD has been organized in the framework of the R2E Mitigation Project, which has the objective to study and mitigate with ad-hoc measures the impact of Single Event Upset (SEU) on the operation of the LHC machine. Electronic components of the LHC accelerator are indeed partly installed in exposed underground areas where significant radiation levels are observed during the normal luminosity runs. The RadMon radiation detector network has been installed to serve as a monitoring and early warning system to protect the concerned electronics and to help to identify in advance critical locations.

RadMon monitors are providing a measure of the high energy (>20 MeV) hadron fluence by counting SEUs in SRAM memories as well as TID (total ionizing dose) using RadFETs at different sensitivities [1]. In locations where high radiation levels are expected (i.e. tunnel zone) the SRAM memories are biased at 5V while in shielded areas - in order to increase their sensitivity - the memories are set to 3V (so that the critical charge necessary to generate a SEU is lower). It has been however observed that the RadMon sensitivity presents a non-linear increase to thermal neutrons when biasing at 3V with respect to 5V. Therefore it is possible [2] to combine RadMon SEU measurement at different voltages to estimate the ratio between the thermal neutron and high energy hadron fluence ( $R = \phi_{th}/\phi_{HE}$ ). RadMons are usually located in critical areas of the LHC: in particular they are covering the triplets, the LSS, UJs and the

RRs. Also the DS and part of the ARC are covered; for these last locations the RadMons are positioned between the last MB and the MQ of a given cell. Usually the RadMon coverage reach only cell 10, apart for some specific points, like for example right of IP2, where the detector are installed with this scheme up to cell 20.

In the general context of the R2E Project activities, we assume that part of the SEUs are caused either by charged hadrons with energy above  $\sim 20$  MeV or by neutrons above few MeV; however another part of SEUs are induced by thermal neutron capture process on light element (such as  $^{10}\text{B}$ ) which might generate light recoils and  $\alpha$ -particles which contribute to the release of energy in the semiconductor. The contribution of HEH and thermal neutrons to the RadMon signal in a mixed radiation field environment can be determined if the energy spectrum – i.e. the R factor - is known, either by using dedicated FLUKA Monte Carlo calculation or by using RadMons operated at different voltages. In the case of LHC environment, the R factor can vary from  $\sim 1$  (tunnel location) to roughly  $\sim 150$  (shielded areas) and therefore its knowledge is of paramount importance if HEH fluence are to be evaluated by using the SEU counts from the RadMons SRAM memories.

The objective of this MD has been to measure the R-factor for tunnel location, between the MBC and the MQ interconnect as well as underneath the MBC dipole, close to the QPS DYPB.C14R2 equipment. Other measurements have been taken during nominal operations of the LHC machine in various locations [3]. In order to achieve the losses necessary to produce the required radiation field, an orbit bump peaking at the MCBH.14R2.B1 (up to  $-24\text{mm}$ ) has been realized, with the beam in inject and dump mode.

Another objective of the present MD is to evaluate the radiation levels and gradient along the length of the cell, both with the RadMons as well as the BLMs; in particular one important parameter for the monitoring of the LHC radiation levels is indeed the extraction of the ratio between the RadMon SEU counts and the dose measured from the BLM located at beam axis. Thanks to the capillarity of the BLM location all around the LHC (RadMon are only partially covering the ARC) this value could be used to extract the HEH fluence in locations where the RadMon SRAM are not installed and this has a significant importance to measure the radiation induced by beam-gas.

## **2. Test area preparation and monitoring upgrades**

The MD has taken place in cell 14R2, which was chosen due to the fact that the same location has been used several times for quench tests as well as because the first QPS ISO150 communication problem on the DQAMC.C14R2 controller was observed there the 18<sup>th</sup> September 2010 (located on the protection rack DYPB.C14R2 installed underneath dipole MB.C14R2); in order to monitor further events during the next Technical Stop the cell was “upgraded” with an additional RadMon placed on the DQAMC.

Prior to this MD the area was equipped with the standard 3 BLMQI per beam (in the standard ARC configuration, where the BLM are installed on the MQs, see Fig. 3) as well as with a FIP RadMon installed underneath the interconnection between the MBC and the MQ. In order to improve the coverage of the radiation field monitoring additional 5 RadMons were installed in the zone as well as two mobile BLM devices (BLMMI), installed at ground level very close to the RadMons. Due to the constraints related to the installation of cables in the tunnel, only two RadMons where of the FIP type (i.e. capable of remote online readout); the

other RadMons where of the “battery-driven” type, which can only be read with an in-situ intervention.

The FIP RadMons were installed (see Fig. 1) where the maximum fluence was expected (the 2RM20S) and on top of the QPS DYPB equipment (2RM10S) in order to spot out critical radiation levels which might have eventually affected the QPS communication system. In order to investigate the R factor values at these two locations, the battery-driven RadMons STD0020 and STD0021 were installed at this very same spot. RadMon STD00022 was indeed installed upstream of the bump maximum towards the end of the MBB of C14R2 while STD0023 was installed underneath the interconnection between the MQ.C14R2 and the MBA.C15R2, to monitor the HEH fluence of the secondary shower produced by the pilot beam on the magnet.

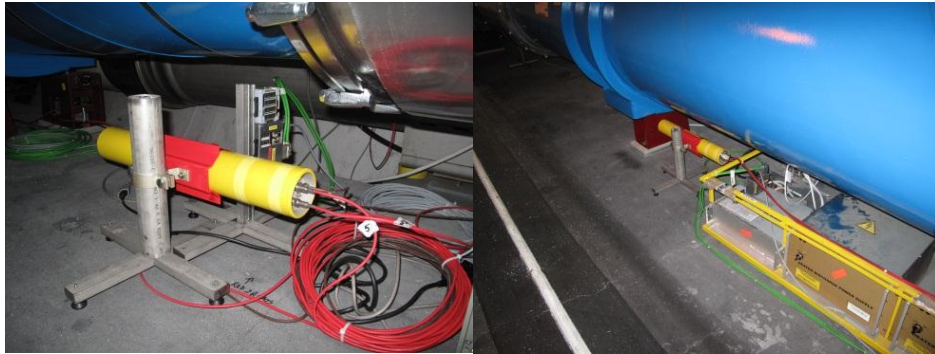


Figure 1: Picture showing the location and installation of the FIP RadMons together with the mobile BLMs (BLMM) installed for the purpose of this MD.

Figure 2 shows an overview of the monitor configuration in cell 14R2 at the moment of the R2E-MD, with the positions of the FIP RadMon at 5V (as green dots), battery-driven RadMon at 3V (as red dots), battery-driven RadMon at 5V (blue dots) and the mobile and fixed BLMs (BLMMI are the mobile BLMs installed close the RadMons and BLMQI are the BLMs installed at beam height). The detailed configuration of the BLMQI together with their expert names is reported in Figure 3.

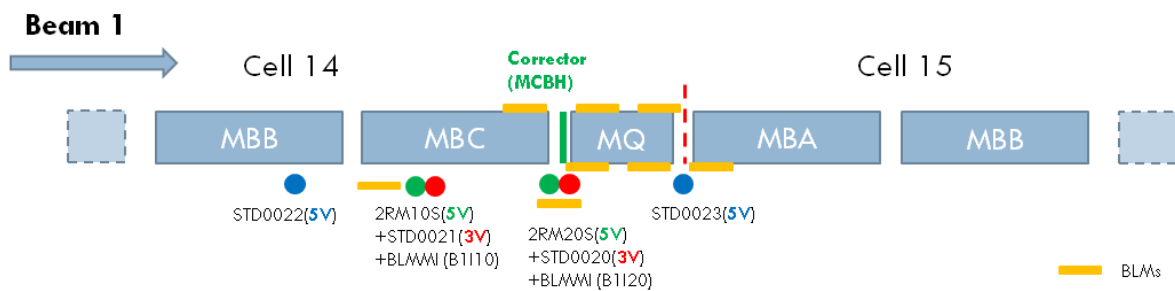


Figure 2: Schematic representation of the configuration of cell C14R2 at the moment of the R2E-MD, including BLMs and RadMons.

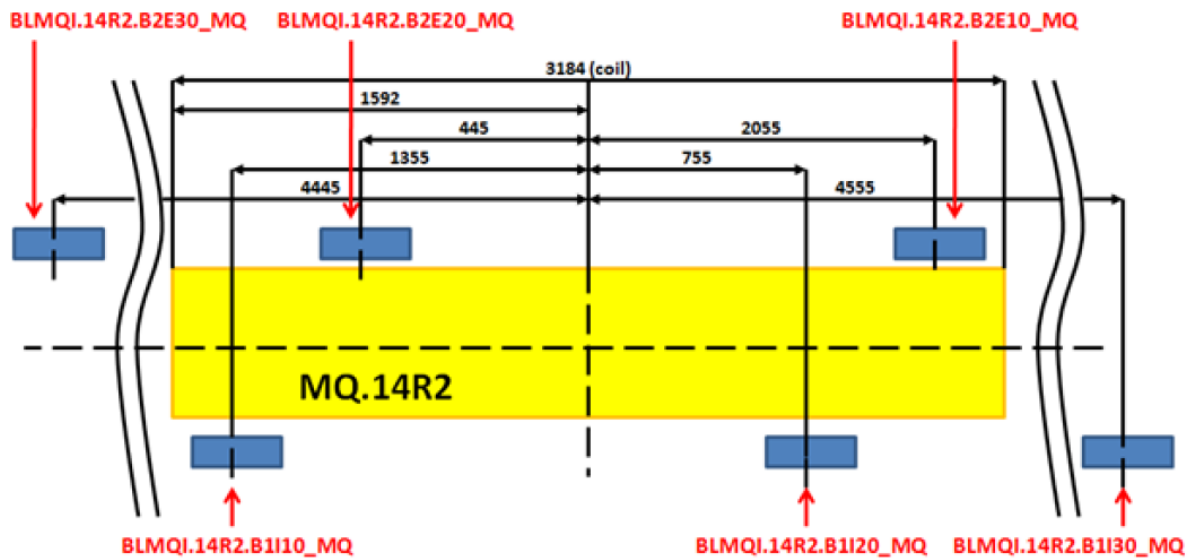


Figure 3: Schematic representation of the BLM installed around the MQ of C14R2 (BLMQI.14R2) [4].

The horizontal 3-correctors bump was foreseen to peak at position 14R2 with a maximum amplitude of -24 mm (inward towards the inner part of the tunnel, see Fig. 4) and applied to beam 1, with beam intensities ranging between  $5 \cdot 10^9$  p/bunch and  $10^{10}$  p/bunch in inject and dump mode. Tests performed during September 2010 in a similar configuration showed that for this bump configuration, no quench was induced even with  $8 \cdot 10^9$  p/bunch. Nevertheless during the setup of the MD the bump was set erroneously to +24mm: with  $7.4 \cdot 10^9$  p/bunch injected into the machine the old QPS of the MBC magnet triggered and the quench heaters fired, leading to the loss of the conditions for sector 23; due to the short period in which the voltage was above the threshold ( $\sim 27$  ms), this event can be classified as the so-called “*quechinos*”-type events.

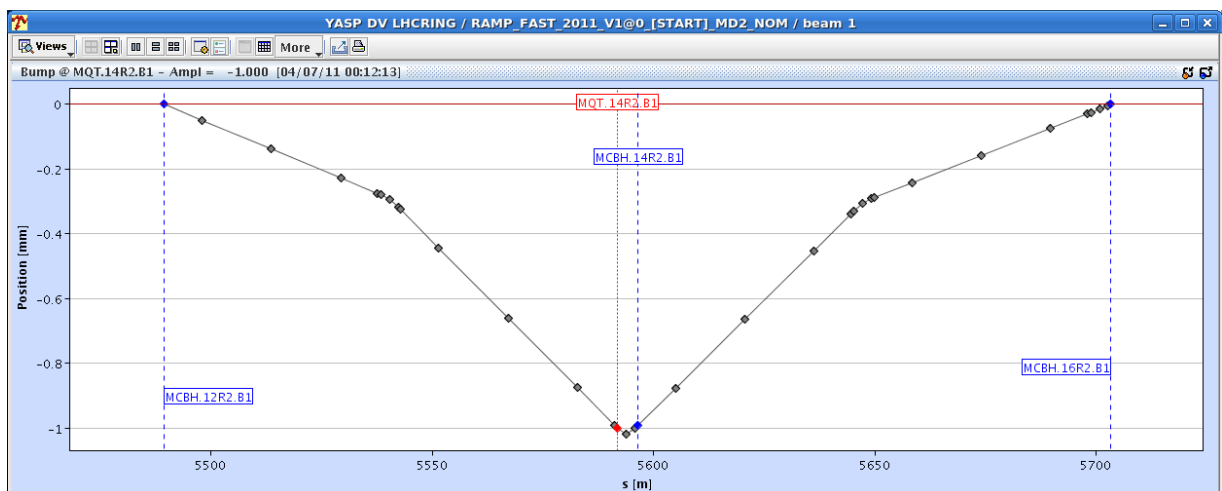


Figure 4: YASP outlook of the bump created on the MCBH.14R2.B1

When the cryogenic conditions came back to nominal the bump was set to -22mm and slowly increased from -22mm to -24mm with bunch intensity up to  $7 \cdot 10^9$  p/bunch; the shower generated by the interaction of the primary protons on the magnet leads to an increase of roughly 10 SEU counts/injection on the 2RM20S RadMon, corresponding to roughly  $\sim 10^7$  HEH/cm<sup>2</sup>/injection. During the course of the night, the local bump was set back again to

+24mm with bunch intensity up to  $6 \cdot 10^9$  p/bunch, but no further QPS trip was observed. Figure 5 shows the evolution of the two FIP RadMon SEU counts over the course of the test; 2RM20S, located below the MBC/MQ interconnect and 2RM10S, located at the beginning of the MBC.

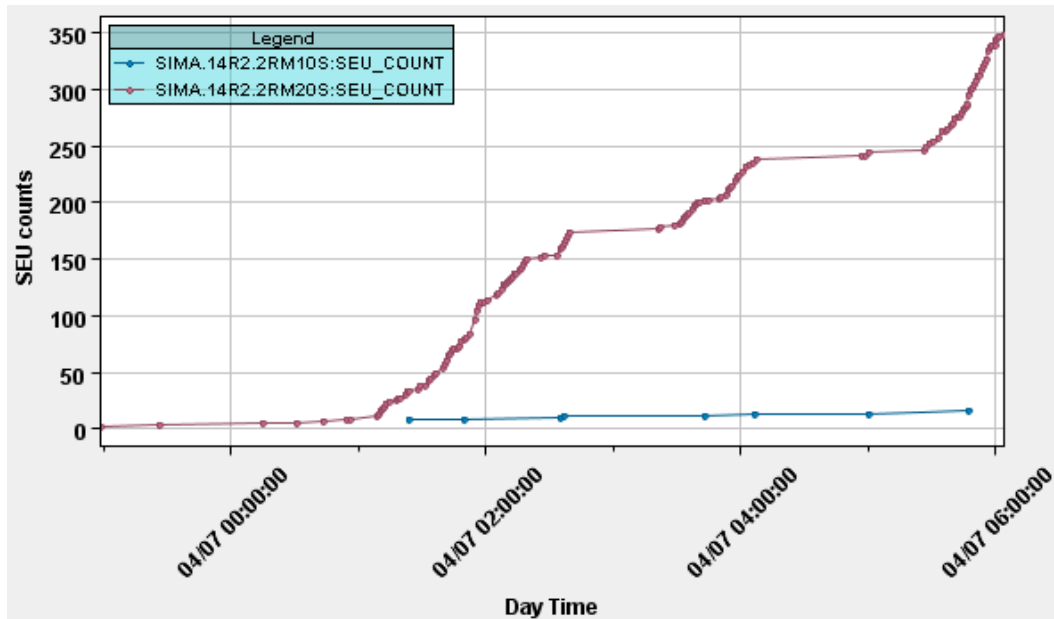


Figure 5: Evolution of the SEU counts from the two FIP RadMon detectors at 5V. RadMon 2RM20S has been installed directly below the MBC/MQ interconnect, while 2RM10S was installed on the QPS DYPB crate upstream the MBC dipole. The significantly higher fluence observed from the 2RM20S gives an indication of the magnitude of the bump.

### 3. R-factor and radiation level gradient investigation

As previously mentioned, the R-factor ( $R = \phi_{th}/\phi_{HE}$ ) is experimentally deduced by the combined use of two RadMons operating at two different voltages, 5V and 3V. In two locations the RadMon were installed in a configuration where the R factor estimation has been possible, namely below the interconnection between the MBC and MQ and the beginning of the MBC where the QPS equipment is in place.

The R factor is extracted according to the following formula [2]:

$$r = \frac{S^{5V} \sigma_{HE}^{3V} - S^{3V} \sigma_{HE}^{5V}}{S^{3V} \sigma_{th}^{5V} - S^{5V} \sigma_{th}^{3V}}$$

$S^{5V}$  and  $S^{3V}$  are the SEU counts measured at 5V and 3V, respectively, while  $\sigma_{HE}^{5V}$  and  $\sigma_{th}^{5V}$  are the SEU cross-section for the RadMon measuring at 5V operating in a high energy hadron field and thermal neutron field, respectively; the same thing apply for  $\sigma_{HE}^{3V}$  and  $\sigma_{th}^{3V}$ , but for a device measuring at 3V. The respective cross-sections are reported in Table 1.

Table 1: The table present the SEU cross section for the RadMons at 5 and 3V for different field types. The cross-sections are extracted with an uncertainty of ~40% depending basically on the chip-by-chip variation [2].

| Field type          | RadMon 5V                                    | RadMon 3V                                    |
|---------------------|--|--|
| Thermal             | $3.1 \cdot 10^{-15} \text{ cm}^2/\text{bit}$ | $1.7 \cdot 10^{-13} \text{ cm}^2/\text{bit}$ |
| High energy hadrons | $3.0 \cdot 10^{-14} \text{ cm}^2/\text{bit}$ | $7.0 \cdot 10^{-14} \text{ cm}^2/\text{bit}$ |

Once the R factor is known, it is possible to deduce, by using either the 5V RadMon or the 3V RadMon, the high energy hadron fluence environment (integrated over the measurement period). In the case of the 5V measurement, the HEH fluence ( $\phi_{HE}$ ) is extracted with the following formula:

$$\phi_{HE} = \frac{S^{5V}}{r \sigma_{th}^{5V} + \sigma_{HE}^{5V}}$$

The results for the different position are reported in Table 2.

Table 2: The table shows – for the different RadMon positions – the extracted R factor with its uncertainties as well as the extracted HEH fluence over the course of the test.

| RadMon (as function of increasing position in the cell) | R factor               | HEH fluence                 |
|---|------------------------|-----------------------------|
| STD0022 (below MBB C14R2)                               | (assumed $11 \pm 10$ ) | $4.5 \cdot 10^6 (\pm 50\%)$ |

|  |                   |                            |
|--|-------------------|----------------------------|
| 2RM10S (below MBC.14R2)                      | 11±10             | 7.5*10 <sup>6</sup> (±50%) |
| 2RM20S<br>(MBC.14R2/MQ.14R2<br>interconnect) | 1.4±0.6           | 6.0*10 <sup>8</sup> (±40%) |
| STD0023 (between MQ.14R2<br>and MBA.15R2)    | (assumed 1.4±0.6) | 3.6*10 <sup>8</sup> (±40%) |

The uncertainty on the R-factor evaluation is essentially dominated in the case of 2RM20S by the uncertainty on the RadMon SEU cross-section evaluation [5], while in the 2RM10S case by a convolution between the effect of low statistics from the RadMon readings as well as from the cross-section uncertainty. The R-factor for the location where the STD0022 and STD0023 are located is assumed to be the same as the value extracted from the contiguous location where FIP RadMon detectors are installed (i.e. the 2RM10S/STD0021 location for the STD0022 and the 2RM20S/STD0020 for the STD0023); this is evidently a brute approximation of the real values.

The higher R-factor extracted from the measurement performed at the 2RM10S location with respect to foreseen values (from simulations and other measurement we expect an R factor in the order of 1-4 for similar locations) could be due to the very local source of radiation during the test (radiation peaking at the level of the MBC/MQ interconnection). In this case, due to the relatively long distance between the MBC/MQ interconnect and 2RM10S, a significant amount of backscattered particles are expected and therefore also a higher thermal neutron fluence to HEH fluence ratio with respect to a standard tunnel location, resembling therefore the spectra of an LHC “shielded-like” area.

#### 4. Comparison between RadMon and BLM

##### 4.1 RadMon SEU counts vs. BLM dose and comparison between the dose at beam height and ground level

As previously mentioned, the knowledge of the RadMon SEU counts/BLM dose ratio is of great support for the evaluation of the cumulated high energy hadron fluence in locations where the RadMon detectors are not installed (such as along the ARC).

Using LHC operational data, by comparing the data between RadMon (located underneath the MB/MQ interconnect of a given cell) and the closest on-axis BLMs located at maximum ~2 meters one with respect to the other, we have established an “operative” SEU counts/dose ratio, corresponding to roughly 1 SEU count (@5V)/mGy (±50%) [3]. Based on this ratio and on the assumption that changes in beam operation do not significantly modify the established relation, it is possible to evaluate the cumulative HEH fluence for specific period of operation (i.e. scrubbing run).

A similar comparison has been performed during the R2E-MD, taking advantage of the configuration between RadMon 2RM20S and BLMQI.14R2.B1I10 (in “LHC-like” standard configuration) and between 2RM20S and BLMMI.14R2.B1I20 (RadMon and BLM one close to each other at tunnel ground level); the results of this analysis are shown in Table 3, for the full duration of the MD test (including the three different MD bump conditions).

Table 3: the table show the cumulative readings from the RadMon SEU counts (at 5V) and the cumulated BLM dose from the mentioned detectors.

| RadMon counts (@5V) | BLM cumulated dose          | Ratio                     |
|---------------------|-----------------------------|---------------------------|
| 345 (2RM20S)        | ~110 mGy (BLMMI.14R2.B1I20) | <b>3.1 SEU counts/mGy</b> |
|                     | ~325 mGy (BLMQI.14R2.B1I10) | <b>1.1 SEU counts/mGy</b> |

The results shows that in the case of an LHC-like configuration (RadMon at 5V underneath the interconnection and closest BLM at MQ location), the results are compatible with those found during normal operation, i.e. ~1 SEU counts/mGy; on the contrary for a BLM installed at ground level - roughly for the same cell longitudinal position – the dose is ~three times lower, yielding to a RadMon SEU counts/BLM dose ratio of ~3 SEU counts/mGy. The factor of 3 reductions in dose when going from beam axis to ground level was already predicted by FLUKA simulations (see Fig. 6 and [6]); the experimental evidence of this gradient gives additional confidence in evaluating the dose and HEH fluence received by equipment located below the tunnel dipoles/quadrupoles by means of the BLMs integrated dose.

The confirmation of the experimentally validated SEU counts/BLM dose is of particular importance because it give an information on the sensitivity with which we are able to predict HEH fluence by using the BLM cumulated dose: the procedure of offset-subtraction performed by the BE/BI team on the BLM data is capable of obtaining cumulative dose values down to few mGy/year (very close to BLM background level). This means, depending on the R-factor value of the particular location under consideration, that we are able to predict cumulated HEH radiation levels from  $2 \cdot 10^6$  HEH/cm<sup>2</sup> (for an R factor of 1) or  $2 \cdot 10^5$  HEH/cm<sup>2</sup> (for an R factor of 100).

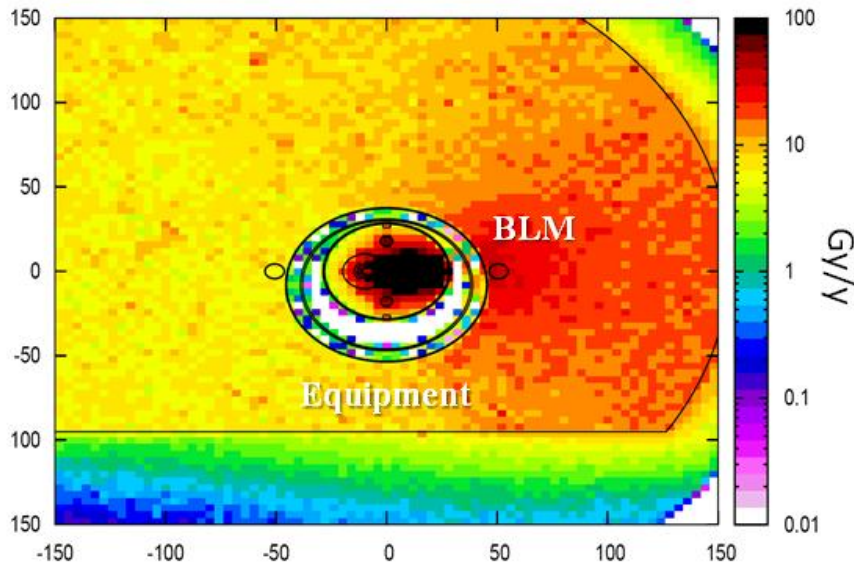


Figure 6: The plot shows a FLUKA simulation of the beam1-gas induced radiation dose around MBB8. The average ratio between BLM location (beam axis) and the equipment below the dipole is around ~3 [6].



## 4.2 RadFET dose compared with BLM-extracted dose

Thanks to the two 400nm and 1000nm RadFETs (MOS Field Effect Transistors) installed on the RadMon device and by using the BLM-measured radiation gradient between beam axis and ground levels, it is possible to compare the dose measured by the RadFET to the one evaluated by the BLMs. The RadFETs are calibrated by using  $\gamma$ -sources in dedicated installations and provides information on the dose in silicon.

It is worth mentioning that as the dose measured by RadFETs is in silicon (compared to nitrogen in case of the BLMs), one has to take into account a ~30% expected difference between the two cases detectors. As it is reported in Table 4 the dose measured by the RadFET is in all cases at the lower edge of its sensitivity (~10 mGy) and therefore non-linearity and big uncertainties are to be expected; where no data is reported (i.e. “N/A”) the RadFETs measurement is below threshold or not installed on the corresponding RadMon.

Nevertheless, even with the above mentioned uncertainties, a reasonable agreement between the dose evaluated by STD0020 and BLMMI.14R2.B1I20 (both of them at ground level) and the dose evaluated by STD0023 and BLMQI.14R2.B1I30 (same longitudinal distance, ground vs. beam axis) is observed (see Table 4). In order to cross-check the readings from the two detectors, further checks at other installations such as H4IRRAD, where higher dose can be achieved in a controlled way – is suggested.

Table 4: Comparison between the BLM dose (in N<sub>2</sub>) cumulated over the course of the MD and the dose measured by the RadMon RadFETs (in silicon).

| <b>BLM</b>       | <b>Total BLM (offset corrected)</b> | <b>RadFET dose (RadMon)</b>                                |
|------------------|-------------------------------------|--|
| BLMMI.14R2.B1I10 | 2 mGy                               | N/A  |
| BLMMI.14R2.B1I20 | 110 mGy                             | 90 mGy<br>(STD0020/2RM20S)                                 |
| BLMQI.14R2.B1I10 | 325 mGy                             | N/A  |
| BLMQI.14R2.B1I20 | 155 mGy                             | N/A  |
| BLMQI.14R2.B1I30 | 70 mGy                              | ~60 mGy (including the 3x<br>gradient factor<br>(STD0023)) |
| BLMQI.14R2.B2E10 | 25 mGy                              | N/A  |
| BLMQI.14R2.B2E20 | 72 mGy                              | N/A  |
| BLMQI.14R2.B2E30 | 65 mGy                              | N/A  |

## 5. Observed ISO-150 Resets and Estimated Failure Cross-Section

During the course of the MD tests we got 8 QPS post-mortem (PM) events (events for which the QPS DAQ gets stalled by a permanent logic low-state on the trigger input – “QPS Ok lost”, without quench heater firing) plus 1 *quenchino* event, during the +24mm initial bump, in which indeed the quench heaters fired; the references of these events in the PM is available in Table 5. Assuming that the QPS ISO150 equipment received  $\sim 7.5 \cdot 10^6$  HEH/cm<sup>2</sup>, its failure cross-section is estimated to be  $\sim 1 \cdot 10^{-6}$  cm<sup>2</sup>. A detailed analysis of these events (whether due to SEU or not) is being performed by TE/MPE, responsible for the equipment; however, given the fact that PM was not observed before 23h20 July 3<sup>rd</sup> and after 06h00 July 4<sup>th</sup>, the possibility that these events are indeed radiation-induced is relatively high.

A previous analysis, performed by using the LHC normal operation data in 2010/2011 (up to April 2011) and by cumulating events occurred in different areas (and therefore in different radiation fields) [7], showed an average equipment failure cross-section of  $1 \cdot 10^{-8}$  cm<sup>2</sup>. This discrepancy (factor of 100 (!) more sensitive to failure) might indeed come from the different radiation field present during standard LHC operation with respect to the one available during the MD test (more thermal neutrons in the latter case with respect to nominal operation) or from the fact that the operational-LHC data comes from an average of events observed during different field conditions (mainly from DS of P1/5/8 (luminosity driven) and DS of P3/7 (collimator losses driven)). It might also be that the failure cross-section of the ISO150 isolator of the QPS system is strongly dependent on the thermal neutron component, significantly more present at the DYPB location during the present MD test as compared to the HEH fluence. In order to address this question, a test in an irradiation facility like H4IRRAD or CNRAD would be needed.

Table 5: the table shows the list of QPS PM events observed during the course of the MD test, with the corresponding timing and PM reference.

| <b>Date</b> | <b>Hour</b> | <b>PM reference</b>     |
|-------------|-------------|-------------------------|
| July 03     | 23h25       | 110703-232539.092_C14R2 |
| July 04     | 01h39       | 110704-013912.681_C14R2 |
|             | 01h55       | 110704-015536.682_C14R2 |
|             | 02h05       | 110704-020527.081_C14R2 |
|             | 02h16       | 110704-021606.681_C14R2 |
|             | 03h48       | 110704-034846.282_C14R2 |
|             | 04h00       | 110704-040015.082_C14R2 |
|             | 05h36       | 110704-053611.481_C14R2 |
|             | 05h57       | 110704-055730.682_C14R2 |

## 6. Observations on the BLM left/right asymmetry

During a previous LHC MDs it has been found that in case of horizontal bump in cell 14R2 it is more likely to quench the upstream MB magnet rather than the MQ magnet, while in

case of vertical loss the MQ magnet quenches first. In order to investigate this unexpected behaviour it has been decided to try to observe the asymmetry between bumps directed inwards (negative, tried in previous MDs) and outwards (positive, not investigated before) of the machine.

By mistake the first created bump was positive (+24 mm) and generated a *quenchino*-type event of the MB magnet at 23:25:40. The injected beam intensity was 0.74E10 protons. After this event it took about 3 hours for the sector to recover. It has been decided not to precycle the magnets, therefore the trajectory of the beam afterwards, even if corrected, could be different than for this event, which could explain the subsequent observations.

After few hours of inject and dump with the -24mm bump, between 3:36 and 3:40 5 shots with bump of +24 mm were performed. Three of them had beam intensity higher than the first shot which quenched the magnet, but this time no quench occurred. Significant numbers of shots with -24 mm bump have been produced afterwards, but again no quench took place for these shots. This behaviour was expected from the results of 2010 MDs.

Figure 7 presents the distributions of BLM signals normalized to the shot intensity for the three loss cases (+24mm which quenched (red), +24mm which did not quench (black) and -24mm (blue)). The distributions are normalized to number of shots (so for the quench event the fraction of events always one, as only one event of this kind has occurred). The first conclusion from this figure is that the negative and positive bumps can be clearly distinguished. On the other hand the BLM signals are very similar for all the +24 mm bump events, and the quench event has no particular signal pattern.

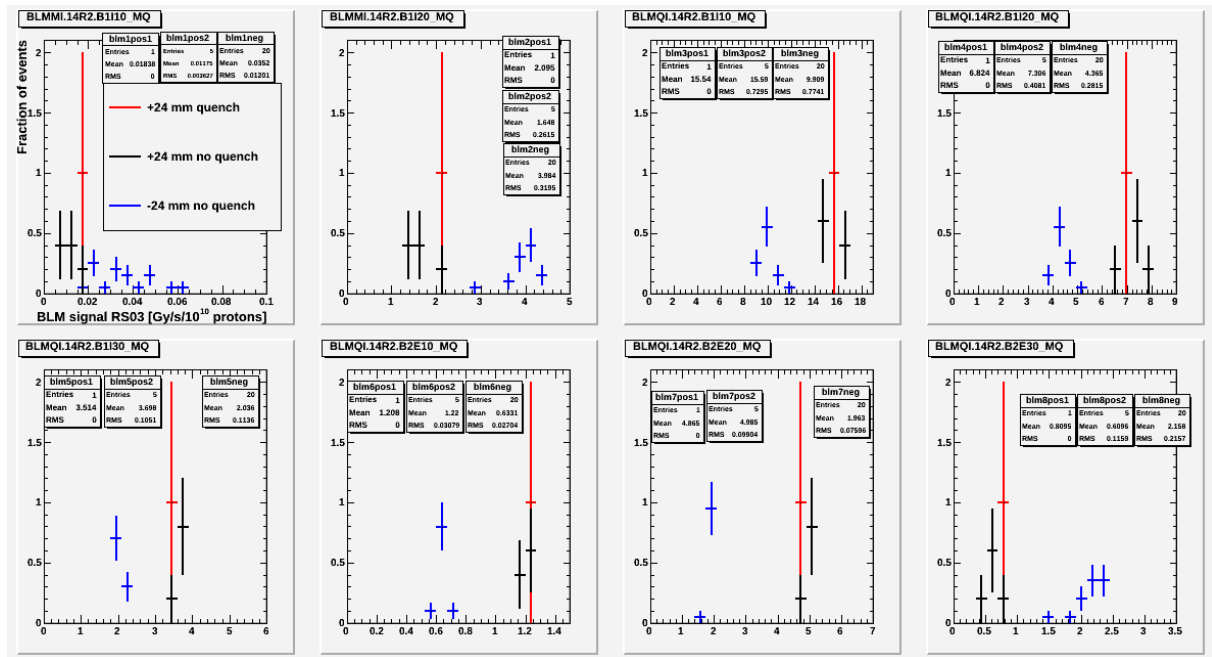


Figure 7: BLM signals normalized to injected beam intensity. The distributions are normalized to number of events so that they correspond to event frequency.

A closer look at the Figure 7 reveals another feature which cannot be understood without performing detailed simulations of the configuration of these events: the BLM signals in the monitors installed on the beam axis of beam 1 always register higher signal when the bump is positive, i.e. in the direction opposite to the BLM location. The same is observed for the beam 2 BLMs installed downstream the corrector magnet (seen as beam 1). On the contrary, the two

mobile BLMs and the single BLM on beam 2 axis (installed on the MB) show higher signals in the case of a negative bump. Further studies will be needed to clarify these observations.

## 7. Main outcomes of the R2E-dedicated MD

The main outcomes of the R2E-dedicated LHC MD, performed in the night between 3<sup>rd</sup> and 4<sup>th</sup> July 2011, where a loss source has been created by means of an orbit bump in cell C14R2 and by using a pilot beam at injection energy, can be summarized as follows:

- I. The test allowed the extraction of the ratio between thermal neutrons and high energy hadrons fluence for one location between the MBC/MQ interconnection and for another one corresponding to the DYPB QPS location underneath the MBC magnet in C14R2.
- II. The radiation level along the last part of the MBC and on the MQ have been extracted in terms of high energy hadrons; the test pointed out a significant gradient of the radiation level opposite of the beam direction, with a decrease of  $\sim 2$  orders of magnitude over roughly 10 meters. This is due to the point-like losses obtained during the present test.
- III. By using mobile and MQ-fixed BLMs we have established an experimental ratio between RadMon SEU counts and BLM dose, obtaining  $\sim 1$  SEU count per mGy for BLM locations on the beam axis and  $\sim 3$  SEU counts per mGy for the mobile BLM at tunnel ground level. The extracted value is in agreement with the same variable extracted during LHC operation in 2010 and confirms the FLUKA estimated reduction of dose between tunnel ground level and beam axis of a factor of 3. The sensitivity of the BLM to low doses also allows estimating the HEH fluence down to few  $10^5$  HEH/cm<sup>2</sup> – depending on the value of the R-factor.
- IV. A comparison between the BLM-extracted dose (in nitrogen) and the RadFETs dose (in silicon) have been performed; the agreement between these two variables is within 30/40%.
- V. By observing the QPS post-mortem and assuming that all of them are induced by SEUs in the ISO150 digital isolator, we extracted an operative failure cross-section for the device of  $\sim 1 \cdot 10^{-6}$  cm<sup>2</sup> for the particular conditions of the MD test.

## Acknowledgments

The excellent collaboration and invaluable contribution of the R2E and RadMon teams (EN/STI), of the BLM team (BE/BI) and of the BE/OP LHC and SPS shift crews involved during the test are warmly acknowledged.

## References

- [1] T. Wijnands *et al.*, *An on-line radiation monitoring system for the LHC machine and experimental caverns* (<http://cdsweb.cern.ch/record/1027423/files/p113.pdf>)
- [2] D. Kramer *et al.*, *LHC RadMon SRAM detectors used at different voltages to determine the thermal neutron to high energy hadron fluence ratio*, RADECS 2010 Proceedings (2010)
- [3] Measurement and Calculation Working Group, <https://indico.cern.ch/categoryDisplay.py?categId=3171>

[4] A. Priebe *et al.*, *Preliminary Analysis of the quench test 3-4 July 2011*, Students Meeting, CERN. July 2011

[5] K. Roed *et al.*, RADECS 2011 Proceedings, to be submitted.

[6] R2E workshop – *Radiation Levels due to Beam-Gas an Update*, R2E Workshop June 2010 (<https://indico.cern.ch/getFile.py/access?contribId=10&sessionId=0&resId=1&materialId=slides&confId=93338>)

[7] M. Brugger, *Possible QPS impact during the scrubbing run*, CERN LMC 85, [https://espace.cern.ch/lhc-machine-committee/Presentations/1/lmc\\_85/lmc\\_85f.pdf](https://espace.cern.ch/lhc-machine-committee/Presentations/1/lmc_85/lmc_85f.pdf)